

Using geographically weighted variables for image classification

BRIAN JOHNSON^{*†}, RYUTARO TATEISHI[‡] and ZHIXIAO XIE[†]

[†]Department of Geosciences, Florida Atlantic University, Boca Raton, FL 33431, USA

[‡]Center for Environmental Remote Sensing (CEReS), Chiba University, Chiba, Japan

(Received 22 July 2011; in final form 1 October 2011)

In this study, geographically weighted variables calculated for two tree species, *Cryptomeria japonica* (Sugi) and *Chamaecyparis obtusa* (Hinoki), were used in addition to spectral information to classify the two species and one mixed forest class. Spectral values (digital numbers for each band) of ‘Sugi’ and ‘Hinoki’ training samples were used to predict the spectral values for the two species at other locations using the inverse distance weighting (IDW) interpolation method. Next, the similarity between each pixel’s spectral values and their IDW predicted values was calculated for both of the tree species. The similarity measures are considered to be geographically weighted because nearer training samples have more of an impact on their calculation. The use of geographically weighted variables resulted in an increase in overall accuracy from 82.2% to 85.9% and an increase in the kappa coefficient from 0.740 to 0.795 for a support vector machine classification.

1. Introduction

One property often present in geographic data sets is spatial autocorrelation (O’Sullivan and Unwin 2003). In remote sensing studies, spatial autocorrelation is typically considered in the accuracy assessment sampling scheme to ensure that pixels used for accuracy evaluation (test pixels) are not located too close to training pixels or other test pixels (Congalton 1988). However, this property of spatial autocorrelation may also be useful for image classification purposes. For example, in forests and other natural areas, ground features that belong to a given land cover class (c_i) that are located near one another may have very similar spectral characteristics because they experience similar amounts of rainfall, similar soil properties and so on. Ground features that also belong to class c_i that are located farther away may have quite different spectral characteristics if climate or soil conditions differ. In cases where this assumption is true, traditional classifiers that ignore the spatial locations of training samples may not be optimal. Instead, it may be more appropriate to estimate the spectral characteristics of class c_i at a specific location by weighting nearer training samples more heavily than samples located farther away.

Few remote sensing studies have incorporated the geographic locations of training samples as a variable for classification. Atkinson (2004) used non-centred covariance and inverse distance weighting (IDW) interpolation techniques to determine class probabilities based on the training data (i.e. pixels closer to training samples of a given

*Corresponding author. Email: bjohns53@fau.edu

class are more likely to belong to that class than another), and the probabilities were used in addition to spectral information for a k -nearest neighbour classification. This approach was able to increase classification accuracy in a simulated image containing three types of land cover. Atkinson and Naser (2010) used a similar methodology to classify an IKONOS image, and classification accuracy also increased when the locations of training samples were considered. Using the geographic location of training samples to estimate class probabilities for each pixel is likely to work well if there are sufficient training samples to accurately represent the spatial configuration of the landscape. However, in heterogeneous landscapes where many types of land cover may be found within a small geographic area, predicting that a pixel is likely to belong to the same class as a nearby training sample may cause classification errors unless a large number of training samples are used. On the other hand, predicting the spectral values (pixel brightness values) of a class at each pixel location, based on the spectral values of nearby training samples, does not make any assumptions regarding the spatial configuration of the landscape (i.e. where a specific land cover is likely to be found), but instead assumes that features belonging to a given class will be more similar if they are closer together. This approach should require fewer training samples in a heterogeneous landscape, as long as they are widely distributed throughout the image to allow for interpolation (rather than extrapolation).

In this study, a spatial interpolation technique, IDW, was used to predict the spectral values for two land cover classes based on the spectral values of their training samples. For each pixel, the similarities between the IDW-predicted spectral values for a given class and the actual spectral values of the pixel were used as additional inputs for image classification. The underlying principle of this design is that, if the spectral signature of a land cover class varies spatially, the use of these similarity variables should increase the classification accuracy because nearby training samples are more heavily weighted for classification. The proposed methods were used to classify two tree species and one mixed forest class using 15 m spatial resolution multispectral Advanced Spaceborne Thermal Emission and Reflection Radiometer (ASTER) data.

2. Study area and data

The study area for this article was a forested area in Ibaraki Prefecture, Japan (36° 57' N, 140° 38' E), approximately 13 km × 12 km. The landscape consists mainly of *Cryptomeria japonica* (Sugi, or Japanese Cedar) planted forest, *Chamaecyparis obtusa* (Hinoki, or Japanese Cypress) planted forest and mixed deciduous broadleaf natural forest, with a small amount of other land use/land cover types scattered throughout the image (agriculture, roads, buildings and so on). Each of the three forest types has different economic uses and environmental conservation values, so accurate mapping of their locations is important for economic and ecological studies. Readers may refer to Kodani (2006), Yamaura *et al.* (2009) and Miyamoto *et al.* (2011) for an overview of the economic and conservation issues related to the forest types found in the study area.

Orthorectified ASTER imagery was acquired for three dates in different seasons (26 September 2010, 19 March 2011 and 8 May 2011) to provide adequate spectral discrimination between coniferous and deciduous tree species. Although the acquired images had been orthorectified, pixels in the September image were still offset by about 15–30 m from corresponding pixels in the other two images. To prevent classification errors caused by misaligned pixels, we further georectified the 26 September image using ground control points until the misalignment was less than 15 m (one pixel).

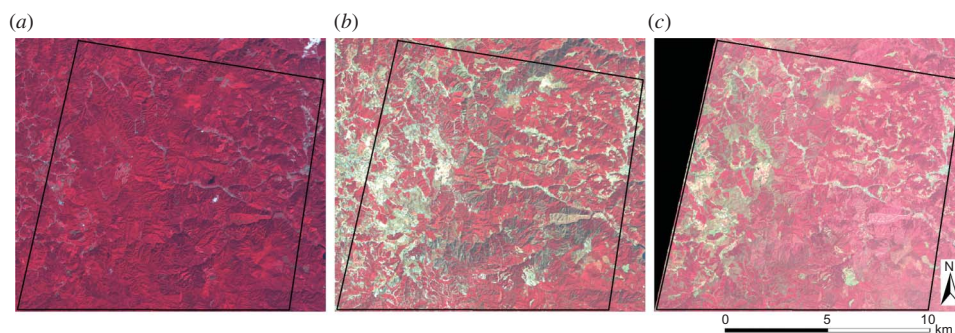


Figure 1. 26 September 2010 (a), 19 March 2011 (b) and 8 May 2011 (c) ASTER false colour composite images of the study area located in Ibaraki Prefecture, Japan, with the study area indicated by the black lines. The centre of study area is located at $36^{\circ} 57' \text{ N}$, $140^{\circ} 38' \text{ E}$.

Since we were mainly interested in reflected spectral information rather than thermal information, only the green ($0.52\text{--}0.60 \mu\text{m}$), red ($0.63\text{--}0.69 \mu\text{m}$) and near-infrared (NIR) ($0.76\text{--}0.86 \mu\text{m}$) bands from each image were used for analysis (total of nine bands, 15 m spatial resolution). Colour infrared images from the three dates are shown in figure 1.

3. Methods

3.1 Training data

Training polygons (about 50 for each class) were digitized for four land cover classes: ‘Sugi’, ‘Hinoki’, ‘mixed broadleaf’ and ‘other’. High-resolution Google Earth imagery from multiple dates was used to assist with the training data digitization (imagery was available for 20 October 2009 and 12 March 2011). Since the classification method used in this study involves spatial interpolation of values from the training samples, pixels located far from training samples may have less accurate predicted values. To minimize classification errors due to this problem, we made sure that training samples for each class were distributed throughout the entire image. The ‘Sugi’ and ‘Hinoki’ classes each consisted of a single tree species, while the ‘mixed broadleaf’ and ‘other’ classes consisted of a mixture of land covers (i.e. different deciduous tree species for the ‘mixed broadleaf’ class, and different types of land use/land cover for the ‘other’ class). Interpolation of spectral values was only performed for the ‘Sugi’ and ‘Hinoki’ classes because problems may arise if the spectral values of a mixed class are interpolated to predict the values at other locations. For example, one training sample for the ‘mixed broadleaf’ class may consist of pixels of a single broadleaf tree species, whereas another nearby training sample may consist of pixels of a different broadleaf species or a mixture of several different broadleaf species. Interpolating the spectral values of the two training samples may not produce accurate predictions because the samples are composed of different tree species. Similarly, interpolating the spectral values for the ‘other’ class is unlikely to produce accurate predictions because training samples can represent ground features with very different spectral characteristics (e.g. agricultural fields, roads, bare soil).

3.2 Calculating geographically weighted variables for classification

IDW is a spatial interpolation method that considers the values of nearby samples to predict the value at a given location (Lam 1983). Nearer samples are assigned greater weights for prediction, and an IDW exponent value controls the rate at which weights decrease as distance increases (i.e. a large IDW exponent value assigns lower weights to distant points than an exponent value close to 1.0). Readers may refer to O'Sullivan and Unwin (2003) for more details about the IDW equation. Other interpolation methods may be used, but the IDW method was chosen for illustration simplicity because it requires less parameter calibration than other methods such as Kriging (only the IDW exponent value needs to be adjusted). The mean spectral values for each band of the Sugi and Hinoki training polygons were used to create 15 m resolution surfaces containing the predicted spectral values for each class. In total, nine 'Sugi' prediction surfaces and nine 'Hinoki' prediction surfaces were created, one for each of the nine spectral bands. We used the nearest 15 training samples to a given pixel for IDW interpolation in an attempt to balance between using too few and too many training samples. We tested many IDW exponent values between 1.00 and 3.00, and the optimal IDW exponent value (rounded to two decimal places) for each band of the 'Sugi' and 'Hinoki' classes was determined by cross-validation of the training data to identify the lowest root mean square prediction error (RMSPE). As an example, the IDW prediction surfaces for the NIR band of the 'Sugi' and 'Hinoki' classes for the 8 May 2011 image are shown in figure 2.

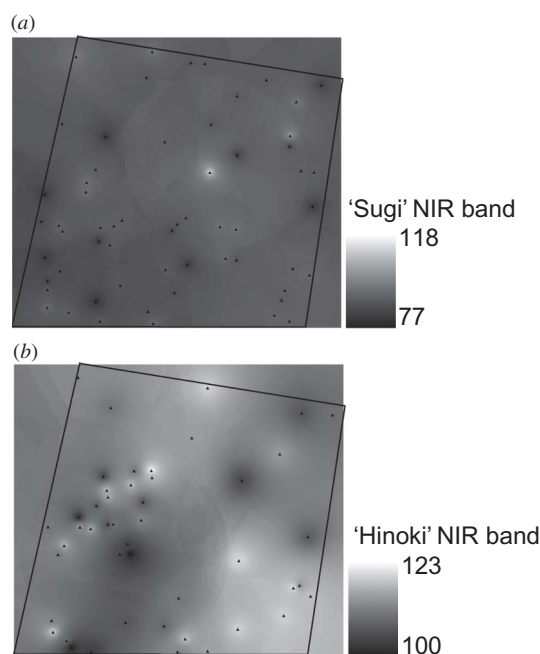


Figure 2. Predicted NIR DN values for the 8 May 2011 image interpolated from the training data using the IDW method. (a) Sugi and (b) Hinoki. Optimal IDW exponent value for this band was 1.00 for Sugi and 1.62 for Hinoki. Locations of training polygons are shown as black triangles.

The predicted spectral values alone may not be very useful for classification if the actual spectral values of each pixel are also not taken into account. For example, at one pixel location, ‘Sugi’ may have a predicted value of 130 for the NIR band in the May 2011 image, but unless the actual spectral value of the pixel is also considered, this predicted value is of little use for classification purposes. However, the degree of similarity between the predicted spectral values for a class and the actual spectral values at a given pixel location may be a useful variable for classification. For example, a pixel with spectral values similar to the ‘Sugi’ predicted values is likely to be Sugi. To determine how similar actual pixel values were to IDW-predicted values for the ‘Sugi’ and ‘Hinoki’ classes, we simply subtracted the actual spectral values from the predicted spectral values (*predicted–actual*) for both of the classes, for each of the nine bands. The result was 18 new variables for classification. These 18 geographically weighted similarity variables were used in addition to the actual spectral values of each pixel (digital number (DN) for each of the nine bands) for classification.

3.3 Image classification

Support vector machines (SVMs), a non-parametric classification algorithm, were used to perform image classification. SVM is a statistical learning algorithm that aims to identify the optimal decision boundary between classes to minimize misclassification (Burges 1998). Prior to classification, a kernel is typically applied to the input feature space to increase the separability between classes. Kavzoglu and Colkensen (2009) give an overview of the commonly used SVM kernels in remote sensing and their functionality. In this study, we used SVM with a radial basis function (RBF) kernel for classification because it has achieved higher classification accuracy than other classifiers in previous remote sensing studies (Foody and Mathur 2004, Kavzoglu and Colkenson 2009). With the SVM–RBF classifier, the user can adjust the cost parameter (c) and the kernel spread function (γ) prior to classification. Readers may refer to Mountrakis *et al.* (2011) for a more in-depth review of the use of SVM in remote sensing studies.

In total, 27 variables were used for image classification (9 spectral bands and 18 similarity measures calculated from the IDW interpolated values). For comparison, classification was also performed using only the nine spectral bands. We tested a wide range of paired combinations of c values (1.25^{-2} , 1.25^{-1} , \dots , 1.25^{31}) and γ values (1.25^{-30} , 1.25^{-29} , \dots , 1.25^{25}), and optimal parameters for each of the SVM classifications were selected through cross-validation of the training data. The optimal c value was 1010 for both the 27 and 9 variable classifications, and the optimal γ values were 0.003 and 1.95 for the 27 and 9 variable classifications, respectively.

3.4 Accuracy assessment sampling scheme

Pixels were selected for accuracy assessment using a stratified systematic unaligned sampling scheme (Jensen 2005) to ensure that they were dispersed across the entire image. A 1 km \times 1 km vector grid was overlaid on the image, and two random points were created within each grid cell. Pixels at the point locations were chosen for accuracy assessment. Polygon boundaries of the selected pixels were extracted and overlaid on high-resolution Google Earth imagery to identify the appropriate land cover class. Pixels that contained more than one of the classes (i.e. mixed pixels) were assigned to the dominant class found in the pixel.

4. Results and discussion

4.1 Accuracy assessment

Table 1 shows the error matrix for the classifications performed with and without the similarity measures described in Section 3. The results show that when the similarity measures were used for classification, the overall accuracy increased by 3.7% (from 82.2% to 85.9%), and the kappa coefficient increased from 0.740 to 0.795. Producer’s and user’s accuracies also increased for almost every class, with the worst result being a tie in producer’s accuracy for the ‘Sugi’ class. These results suggest that incorporating geographically weighted variables can be useful for image classification in natural environments.

The SVM classified map produced using the similarity measures is shown in figure 3. To identify some of the sources of classification errors, point locations of all misclassified test pixels were overlaid on the imagery. In many cases, we found that the errors occurred along the boundaries of different land cover classes, where pixels contained a mixture of more than one type of land cover. Some errors were also found in pixels covered by shadow, but misclassification due to shadows was reduced somewhat because images from three different dates were used (most pixels were in direct sunlight in more than one of the images).

4.2 Effects of feature selection using Moran’s I

To see if accuracy increased further when feature selection was employed, we tested the spectral values of the ‘Sugi’ and ‘Hinoki’ training samples for spatial autocorrelation

Table 1. Confusion matrices for the SVM classifications.

Classification						
Reference data	S	H	D	O	Total	PA (%)
(a) SVM classification with geographically weighted similarity measures						
S	122	11	3	0	136	90
H	4	34	0	0	38	89
D	7	3	88	7	105	84
O	1	0	10	35	46	76
Total	134	48	101	42	325	
UA (%)	91	71	87	83		
Overall accuracy						85.9
Kappa coefficient						0.795
(b) SVM classification without geographically weighted similarity measures						
S	122	12	2	0	136	90
H	8	30	0	0	38	79
D	11	3	82	9	105	78
O	1	0	12	33	46	72
Total	142	45	96	42	325	
UA (%)	86	67	85	79		
Overall accuracy						82.2
Kappa coefficient						0.740

Note: S, Sugi; H, Hinoki; D, mixed deciduous broadleaf; O, other; PA, producer’s accuracy; UA, user’s accuracy.

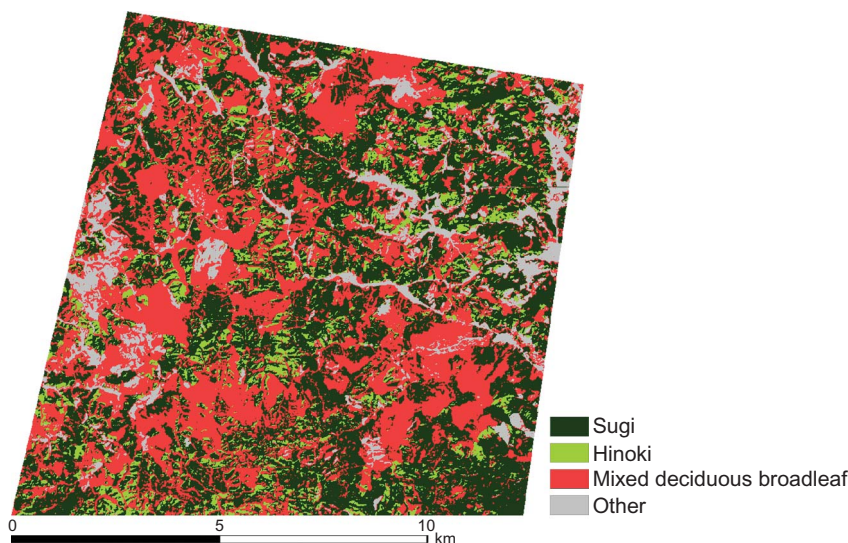


Figure 3. SVM classified map produced when the geographically weighted variables were used in addition to the actual spectral information for classification.

using Moran's I (Moran 1950), a metric that calculates how similar, on average, a sample is to other nearby samples. We then performed another classification using similarity variables only for bands that showed positive spatial autocorrelation at a 95% confidence level ($p < 0.05$). For Moran's I calculations, we used the inverse distance weighting scheme (i.e. all samples considered for calculation, but nearer ones have greater weight) (O'Sullivan and Unwin 2003). For the 'Hinoki' class, spectral values for six of the nine bands exhibited positive spatial autocorrelation with $p < 0.05$ (all three bands from the May image, the NIR and green bands from the September image and the green band from the March image), so only the similarity measures for those six bands were used for Hinoki. For the 'Sugi' class, spectral values exhibited positive spatial autocorrelation ($p < 0.05$) in four of the nine bands (red and green bands from the May and September images). When SVM classification was performed again using the actual spectral values from the nine ASTER bands, the six similarity variables for Hinoki and the four similarity variables for Sugi, results were actually worse than when all 27 variables were used for classification (overall accuracy was 84.3% and the kappa coefficient was 0.773). This suggests that the inclusion of the similarity values for the other bands improved results even though they exhibited weaker spatial autocorrelation.

4.3 Comparison with results of a similar study

The kappa coefficient achieved in this study was a bit lower than that achieved by Ota *et al.* (2011), which used IKONOS imagery, resampled to 15 m spatial resolution, to classify Sugi, Hinoki, mixed forest and clear-cut areas (we estimate their kappa coefficient was 0.85–0.87 based on a line chart; numerical value not reported). However, in the previous study, locations chosen for assessing classification accuracy were all within tree stands at least 1 ha in area, and more than 45 m from the stand edge,

thus avoiding classification errors caused by mixed pixels. Since many classification errors in this study occurred along the boundaries of different types of land cover, the lower accuracy we achieved is probably not indicative of a worse classification result, but rather a more random sampling scheme. Also important to note is that Ota *et al.* (2011) found that the use of texture information led to higher classification accuracy at 15 m spatial resolution, so for future studies, the use of texture information in addition to geographically weighted variables may further increase classification accuracy.

5. Conclusions

In this study, spectral values for Sugi and Hinoki tree species were predicted for all pixels in the study area by spatially interpolating the spectral values of the training samples. The degree of similarity between the actual spectral values of a pixel and the predicted values for the ‘Sugi’ and ‘Hinoki’ classes was calculated for each spectral band. When the similarity measures were used as additional input layers for classification, classification accuracy and the kappa coefficient improved for a SVM classification.

Based on the results of this study, it may be useful to incorporate geographically weighted variables for image classification in forests and other natural areas, especially for classification at the species level. Mixed pixels were difficult to classify when the geographically weighted variables were used for classification, although their use did not seem to cause additional misclassification of mixed pixels. However, great care should be taken to avoid accidentally including mixed pixels in the training samples, as mixed pixels would alter the predicted spectral values for nearby pixels. It should also be noted that, in images that contain rugged topography, additional information, such as predicted solar illumination for each pixel (based on topography, solar zenith angle, solar azimuth and so on), may also need to be considered for predicting the spectral values of a class. For example, topographic correction methods such as those described in Richter *et al.* (2009) could be applied prior to performing IDW interpolation.

In the future, we plan to investigate the effect that distance from training samples has on classification errors to see if pixels located farther from ‘Sugi’ or ‘Hinoki’ training samples experienced more classification errors than nearer pixels. In future studies, more sophisticated spatial interpolation methods, such as Kriging, should be tested to see if accuracy increases further. Additional similarity measures should be tested as well. It is also necessary to test the developed methods in different types of environments and/or using different types of remote sensing data (e.g. high-resolution imagery, hyperspectral imagery or synthetic aperture radar imagery). Finally, the use of additional spatial information, such as image texture, may further improve results.

Acknowledgements

This study was supported by the National Science Foundation (NSF East Asia and Pacific Summer Institutes Fellowship) and the Japan Society for Promotion of Science (JSPS Summer Program). Orthorectified ASTER data were provided by the Land Processes Distributed Active Archive Center (LP DAAC) located at the US Geological Survey (USGS) Earth Resources Observation and Science (EROS) Center (lpdaac.usgs.gov).

References

- ATKINSON, P., 2004, Spatially weighted supervised classification for remote sensing. *International Journal of Applied Earth Observation and Geoinformation*, **5**, pp. 277–291.
- ATKINSON, P. and NASER, D., 2010, A geostatistically weighted k-nn classifier for remotely sensed imagery. *Geographical Analysis*, **42**, pp. 204–225.
- BURGES, C., 1998, A tutorial on support vector machines for pattern recognition. *Data Mining and Knowledge Discovery*, **2**, pp. 121–167.
- CONGALTON, R., 1988, Using spatial autocorrelation analysis to explore errors in maps generated from remotely sensed data. *Photogrammetric Engineering and Remote Sensing*, **54**, pp. 587–592.
- FOODY, G. and MATHUR, A., 2004, A relative evaluation of multiclass image classification by support vector machines. *IEEE Transactions on Geoscience and Remote Sensing*, **42**, pp. 1335–1343.
- JENSEN, J., 2005, *Introductory Digital Image Processing: A Remote Sensing Perspective*, pp. 502–504 (Upper Saddle River, NJ: Pearson Prentice Hall).
- KAVZOGLU, T. and COLKENSEN, I., 2009, A kernel functions analysis for support vector machines for land cover classification. *International Journal of Applied Earth Observation and Geoinformation*, **11**, pp. 352–359.
- KODANI, J., 2006, Ecology and management of conifer plantations in Japan: control of tree growth and maintenance of biodiversity. *Journal of Forest Research*, **11**, pp. 267–274.
- LAM, N., 1983, Spatial interpolation methods: a review. *Cartography and Geographic Information Science*, **10**, pp. 129–150.
- MIYAMOTO, A., SANO, M., TANAKA, H. and NIIYAMA, K., 2011, Changes in forest resource utilization and forest landscapes in southern Abukuma Mountains, Japan during the twentieth century. *Journal of Forest Research*, **16**, pp. 87–97.
- MORAN, P., 1950, Notes on continuous stochastic phenomena. *Biometrika*, **37**, pp. 17–33.
- MOUNTRAKIS, G., IM, J. and OGOLE, C., 2011, Support vector machines in remote sensing: a review. *ISPRS Journal of Photogrammetry and Remote Sensing*, **66**, pp. 247–259.
- O’SULLIVAN, D. and UNWIN, D., 2003, *Geographic Information Analysis*, pp. 28–30, 197–202, 227–233 (Hoboken, NJ: Wiley).
- OTA, T., MIZOUE, N. and YOSHIDA, S., 2011, Influence of using texture information in remote sensed data on the accuracy of forest type classification at different levels of spatial resolution. *Journal of Forest Research*, doi:10.1007/s10310-010-0233-6.
- RICHTER, R., KELLENBERGER, T. and KAUFMANN, H., 2009, Comparison of topographic correction methods. *Remote Sensing*, **1**, pp. 184–196.
- YAMAURA, Y., IKENO, S., SANO, M., OKABE, K. and OZAKI, K., 2009, Bird responses to broad-leaved forest patch area in a plantation landscape across seasons. *Biological Conservation*, **142**, pp. 2155–2165.